〈논 문〉 SAE NO. 98370050

Understanding Automobile Roll Dynamics and Lateral Load Transfer Through Bond Graphs

Sang-Gyun So*, Dean Karnopp**

ABSTRACT

It is clear that when an automobile negotiates a curve the lateral acceleration causes an increase in tire normal load for the wheels on the outside of the curve and a decrease in load for the inside wheels. However, just how the details of the suspension linkages and the parameters of the springs and shock absorbers affect the dynamics of the load transfer is not easily understood. One even encounters the false idea that since it is the compression and extension of the main suspension springs during body role which largely determines the changes in normal load, if roll could be reduced, the load transfer would also be reduced.

Using free body diagrams, one can explain quite clearly how the load is transferred for steady state cornering, and, using complex multibody models of particular vehicles one can simulate in good fidelity how load transfer occurs dynamically. Here we adopt a middle ground by using the concept of roll center and using a series of half-car bond graph models to point out main effects. Since bond graph junction structures automatically and consistently constrain geometric and force variables simultaneously, they can be used to point out hidden assumptions of other simplified vehicle models.

1. Introduction

Understanding of automobile dynamics is simplified by initially considering longitdinal lateral and vertical dynamics separa-

* 정회원, Samsung Electro-Mechanics Co. Automotive Products

** Professor, University of California at Davis, Dept. of MAE

tely. The effects of spring and damping rates on ride quality can be at least roughly assessed using a mathematical model of the type used in vibration isolation studies. Similarly the so-called "bicycle" model can be used to describe handling qualities such as oversteer and understeer. In neither model do details of suspension linkages appear nor are the vertical motions of the first model coupled with the lateral motions of the second.

The bicycle model, which combines the two front and the two rear wheels into single front and rear equivalent wheels is capable of accurately representing quasi-steady lateral dynamics if a series of factors can be incorporated in the basic tire lateral force vs. slip angle relationships.[1] These factors involve the suspension kinematics through steering and camber change due to body roll, as well as the effect of lateral load transfer acting through the nonlinear tire characteristics. Thus, to the extent that one can develop an intuitive feeling for how roll magnitude and load transfer are related to various suspension parameters the simple bicycle model can give an idea of how changes are likely to affect handling.

Much more complex but realistic computer models of vehicles are available using multi-body dynamics techniques. These models can predict with good accuracy how a specific vehicle will behave. These models are less successful at explaining why a particular design reacts as it does and thus are not always useful in suggesting changes in a design to correct undesirable behavior. Trial and error experimentation on a very complex model may be faster than trial and error on a real prototype, but without some guiding principles it can also be a frustrating and time consuming process. With the simple bond graph models discussed below, we hope to illustrate fundamental points about roll dynamics and load transfer which should help develop engineering judgment about how suspension changes should effect overall vehicle dynamics. Bond graph techniques are presented in detail in Ref.[5]

2. Combining Vertical and Lateral Dynamic Models

In explaining vehicle dynamics, a variety of models with a restricted number of degrees-of-freedom are typically used.[2,3] A ride model concerned with vertical motion might neglect longitudinal, lateral and yaw motion but include roll, pitch and heave for the body and possibly unsprung mass motion for each wheel. The bicycle type model could include yaw, lateral and possibly longitudinal motion. It seems natural to combine these two models as shown in Fig.1 from.[4]

Note that the spring and damping rates have been reflected out to the wheel locations which is logical for the ride model. There are no anti-roll bars shown and all details of the suspension linkages are absent. Since the roll and pitch angles are small normally, it is fairly straight forward to write the equations for this type of model and it is no problem to include nonlinear spring, damper and tire laws.[4] The advantage of this type of model is that despite the fairly large number of degrees-of-freedom, only a modest number of parameters are needed. There is no need to know what sort of suspension is used at all so

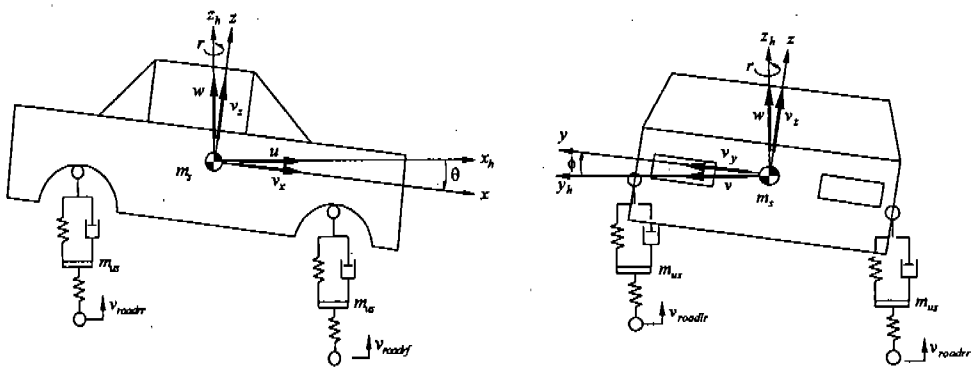

(a) Side view (b) Rear view

Fig.1 Three-dimensional vehicle model for ride and handling, Ref.[4]

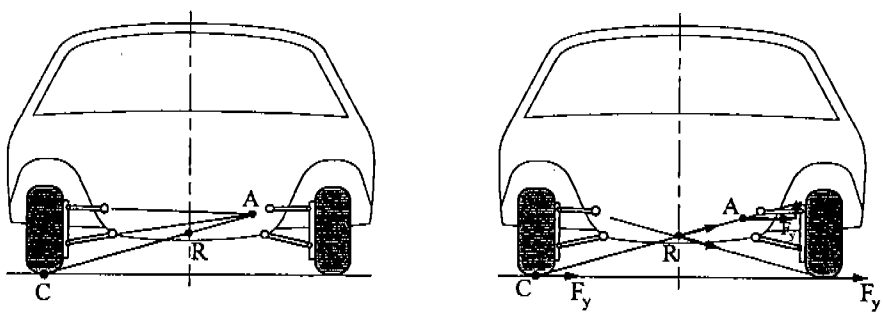

Fig.2 Roll center analysis of an independent suspension, Ref.[2]

none of the many parameters associated with the multiple links and attachment points of modern suspensions need to be specified.

In the models below, we use the concept of a roll center which can be found for a wide variety of suspension type using a basically graphical analysis.[2,3] Fig.2 shows how the roll center is determined for an independent suspension.[2] Although the roll center analysis is only approximate since it doesn't take into account bushing flexibility and is not a point fixed in the vehicle as it rolls, it does bring in details of the various suspension types in a single parameter-the roll center height. Thus, we will analyze what the effect of roll center height has on roll magnitude and load transfer and thus we will be better able to understand how a change in suspension type or linkage angle might affect the vehicle dynamics.

The first question we will address concerns the evident lack of a roll center in Fig.1. Although one could use the complete equations for the three dimensional motion given in Ref.[4], these equations written in a rotating coordinate frame are more complex than necessary to make important observations about roll dynamics.

We first use the model shown in Fig.3. The model concerns only half of the ve-

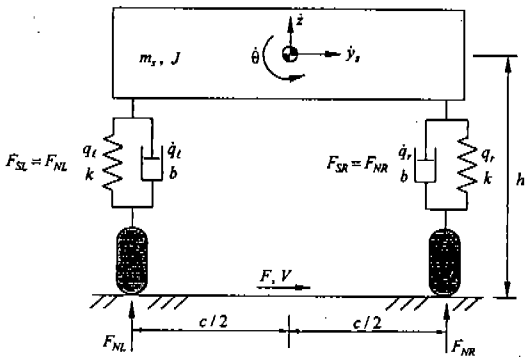

Fig.3 Half-car model corresponding to Fig.1

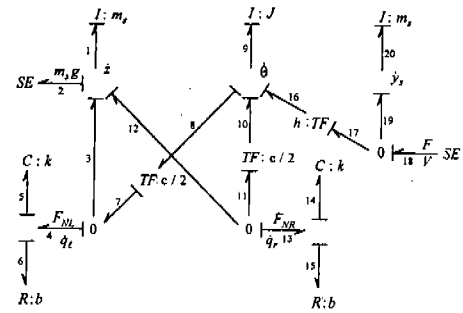

Fig.4 Bond graph for model of Fig.3

hicle and a single axle. Furthermore we treat the vehicle as if it were mounted on a table which could accelerate side-ways. This avoids the use of rotating coordinate systems and approximates the effects of lateral acceleration in high speed turns where the yaw rate is small. The sprung mass is m, and its moment of inertia about the centroid is J. The spring deflections are q_l and q_r and both springs have constants(reflected to the wheel locations) of k. The mass center height about the roadway plane is h, the track is c and the tire normal forces are and F_{NL} and F_{NR}. F represents the sum of the lateral tire forces and V the velocity of the roadway. For the first model, we neglect the unsprung mass.

A conventional analysis using a free body diagram of the sprung mass in Fig.3 yields the following three equations :

$$m_s\ddot{z}=F_{NL}+F_{NR}-m_sg, \tag{1}$$

$$m_s\ddot{y}_s=F, \tag{2}$$

$$J\ddot{\theta}=hF-(c/2)F_{NL}+(c/2)F_{NR}. \tag{3}$$

A bond graph,[5] is easily constructed incorporating these relations.(Those using bond graphs conventionally express the left hand sides of these equations as the rate of change of two linear and one angular momentum rather than as acceleration expressions.) Fig.4 shows three I-elements at the top representing the three inertia terms and their associated 1-junctions sum the forces as required by Eqs.(1)-(3) The three forces appear on the three 0-junctions at the bottom of the graph.

A peculiarity of bond graph junction structures,[5] is that if effort relations are represented, corresponding flow relations are automatically implied. For example, based on the force balances of Eqs.(1)- (3), the zero junctions provide the kinematic relationships.

$$\dot{q}_l=-\dot{z}+(c/2)\dot{\theta}, \tag{4}$$

$$\dot{q}_r=-\dot{z}-(c/2)\dot{\theta}, \tag{5}$$

$$V=\dot{y}_s+h\dot{\theta}. \tag{6}$$

Eqs.(4) and (5) show how the spring and damper relative velocities are related to the sprung mass motion. Eq.(6) is particularly interesting. When we assume the table is not moving, $V=0$, we see that

$$\dot{y}_s = -h\dot{\theta}, \tag{7}$$

which implies that in this model, the effective roll center is at ground level. The bond graph points out that if we use h as the lever arm relating the lateral force to a moment about the center of mass of the body, we also imply that the body is constrained to rotate about a point in the ground plane.

The conclusion is that models of the type of Fig.1 inherently assume that the roll center heights are zero. A pure trailing arm rear suspension has a zero roll center height but most actual suspension designs do not.

It is easy to compute the load transfer in a steady turn. We assume F is constant so the lateral acceleration in our system is

$$a_{lat} = \dot{y}_s = F/m_s. \tag{8}$$

Setting the accelerations to zero in Eqs. (1)-(3) we have.

$$F_{NL} = m_s g/2 + Fh/c, \tag{9}$$

$$F_{NR} = m_s g/2 - Fh/c, \text{ or} \tag{10}$$

$$F_{NL} - F_{NR} = 2Fh/c. \tag{11}$$

For this model without an anti-roll bar, the roll stiffness is due solely to the two springs a distance c apart. The roll stiffness is.

$$K_\theta = kc^2/2, \tag{12}$$

and the roll angle in the steady state is

$$\theta = \frac{2Fh}{kc^2} \tag{13}$$

We note that for steady turns, the load transfer depends only on F(or a_{lat}) and the center of mass height h. The roll angle θ could be reduced by making k greater without affecting the load transfer although this would stiffen the vertical spring constant to the possible detriment of ride quality.

The dampers have no affect on the steady state load transfer but do effect the transient roll response to lateral acceleration changes. The bond graph model yields differential equations which could be used to study dynamic roll and load transfer responses but since the model has no anti-roll bar and presumes a zero roll center height, we will proceed in stages to augment the model to include effects present in real suspension systems.

3. Extended Roll Model Including Finite Roll Center and an Anti-Roll Spring

Fig.5 shows schematically a half-car roll model incorporating a roll center at a distance of h_{rc} above the ground, (this distance could be negative for some sus-

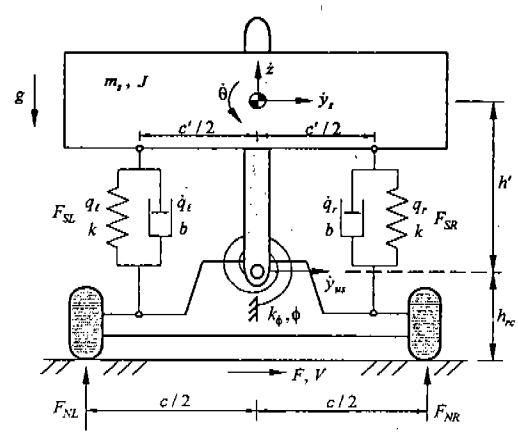

Fig.5 Roll model with finite roll center height and anti-roll bar spring

pension configurations). The effect of an anti-roll bar is represented by a torsional spring of constant k_ϕ. This spring exerts a restoring moment on the body proportional to the angle ϕ(which in this model is identical to the body angle θ) but the spring has no effect on the vertical spring rate.

The spring-damper units are shown at a distance $c'/2$ from the centerline which can be different from the half track $c/2$. The distance h' represents the distance from the roll center to the body mass center. In this model the structure supporting the wheels is considered massless and the wheels are rigid. The internal suspension forces F_{SL} and F_{SR} are no longer identical to the tire loads F_{NL} and F_{NR} except at equilibrium when there is no lateral acceleration.

Note that the lateral velocity of the roll center $\dot{y}_{us}$ is identical with the ground velocity V in this model. Eqs.(1)-(6) remain valid if F_{SL}, F_{SR}, c' and $\dot{y}_{us}$ are substituted for F_{NL}, F_{NR}, c and V and the anti-roll torque is added to Eq.(3). The result is that the bond graph for this model shown in Fig.6 is nearly identical to

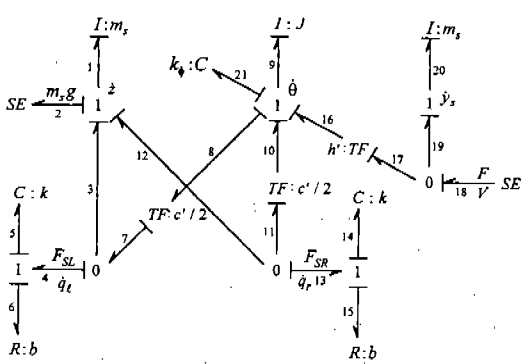

Fig.6 Bond graph for the model of Fig.5.

the one shown in Fig.4 for the previous model except for the extra torsional spring and the change in meaning of some of the variables and parameters.

Results similar to those given in Eqs. (9)-(13) can be found for turn in which F and a_{lat} are constant. First, we note that the roll stiffness corresponding to K_θ in Eq.(12) is now.

$$k_\phi = k_\phi + \frac{k(c')^2}{2} \tag{14}$$

and the steady state roll angle is

$$\theta = Fh'/k_\phi . \tag{15}$$

Thus the anti-roll torque τ is

$$\tau = k_\phi Fh'/K_\phi . \tag{16}$$

Using the new versions of Eqs.(1) and (3) with zero acceleration,

$$F_{SL} + F_{SR} = m_s g, \tag{17}$$

$$F_{SL}(C'/2) - F_{SR}(c'/2) + \tau = Fh', \tag{18}$$

the results are

$$F_{SL} = \frac{m_s g}{2} + \frac{Fh'(k(c')^2/2)}{K_\phi c'} \tag{19}$$

$$F_{SR} = \frac{m_s g}{2} + \frac{Fh'(k(c')^2/2)}{K_\phi c'} \tag{20}$$

$$F_{SL} - F_{SR} = \frac{2Fh'(k(c')^2/2)}{K_\phi c'} \tag{21}$$

These results can be compared to Eqs. (9)-(11) for the simpler previous model. Without the anti-roll spring constant k_ϕ in Eq.(13) the two sets of equations just derived appear to reduce to the previous results at least in form(but not in meaning).

There is, however, an easily resolved

paradox in these results. If one imagined increasing the roll center in Fig.5 until h' vanished, then Eq.(15) predicts no roll angle at all and no load transfer at the suspension forces and would be predicted by Eqs.(19)-(21). This type of thinking is related to the incorrect notion that elimination of body roll eliminates load transfer.

The simple resolution of the paradox involves the observation that the suspension forces are internal to the entire system and are not identical to the external tire load forces. The analysis of Fig.3 which leads to the results of Eqs.(9)-(11) would apply also to Fig.5 if the total height to the center of mass, $h' + h_{rc}$ were used in place of h in Eqs.(9)-(11). There is no way to make $h' + h_{rc}$ vanish for an automobile so there will always be load transfer whether or not there is a roll angle.

Fig.7 shows the result of a simulation using parameters shown in Table 1 of a step lateral acceleration applied to the model of Figs.3 and 4 which gives the total tire normal forces assuming zero roll

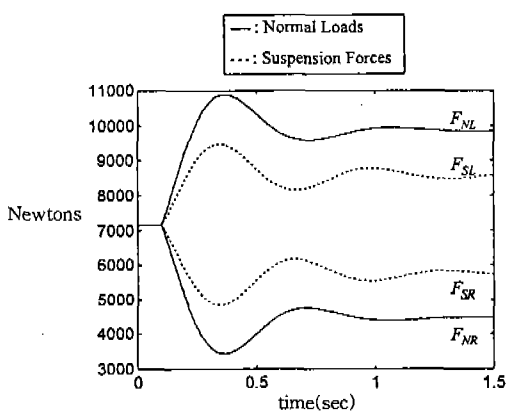

Fig.7 Responses to step in lateral acceleration: F_{NL} and F_{NR} as found from Fig.4, and F_{SL} and F_{SR} from Fig.6

Table 1 Vehicle parameters for simulations

Sprung Mass(m_s)	1,460(k_g)
Left and Right Suspension Spring Stiffnesses(k)	37,460(N/m)
Left and Right Tire Vertical Stiffnesses(k_t)	351,000(N/m)
Track Width(c)	1.516(m)
Sprung Mass Center Height from Ground(h)	0.7(m)
Roll Moment of Inertia(J)	460(K_gm^2)
Unsprung Mass(m_{us})	75.5 (k_g)
Left and Right Suspension Damping Coefficients(b)	2,910 (N-sec/m)
Anti-Roll Bar Spring Stiffness(k_θ)	19,200 (N-m/rad)
Distance between Left and Right Susp. Springs(c')	1.216(m)
Roll Center Height From Ground(h_{rc})	0.2(m)

center height and the model of Figs.5 and 6 which yields only the internal suspension forces with a positive roll center height. In this case, the total height of the mass center in Fig.5, $h' + h_{rc}$ is assumed to be equal to h in Fig.3.

4. Why the Bond Graph Does Not Compute Tire Loads

The same sort of trick can be used to allow computation of constraint forces in a bond graph. In Fig.5, the wheel normal loads play no role since the associated vertical velocities at the wheel location are assumed to vanish. Thus there is no port and no power associated with the normal loads. In Fig.8, ground velocities $\dot{z}_{gl}$ and $\dot{z}_{gr}$ are assumed to exist as if the tires were rolling over an uneven surface.

If we now correctly represent kinematic constraints as was done in Chap.2, using a bond graph junction structure, then the bond graph will automatically compute the corresponding forces. The suspension deflection rates for Fig.8 are more complex than Eqs.(4) and (5).

$$\dot{q}_l = a\dot{z} + \frac{c'}{2}\dot{\theta} + \dot{z}_{gl}\frac{c+c'}{2c} + \dot{z}_{gr}\frac{c-c'}{2c}, \quad (22)$$

$$\dot{q}_r = a\dot{z} - \frac{c'}{2}\dot{\theta} + \dot{z}_{gl}\frac{c-c'}{2c} + \dot{z}_{gr}\frac{c+c'}{2c}. \quad (23)$$

The anti-roll spring angle ϕ is no longer

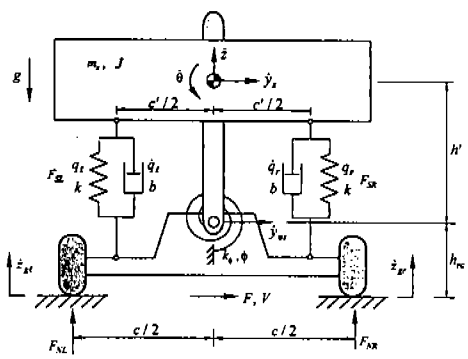

Fig.8 Model of Fig.5 augmented to allow ground motion at both wheels

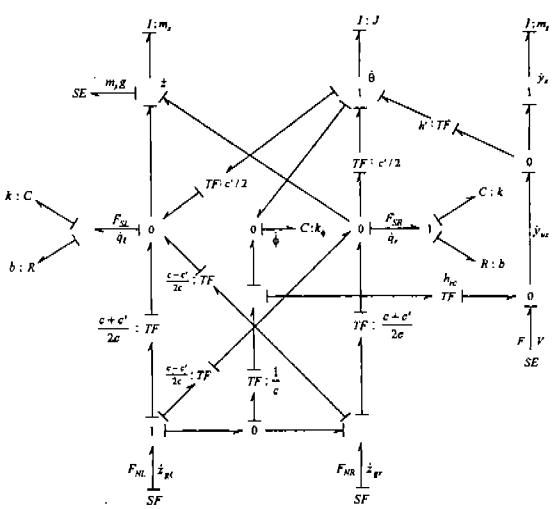

Fig.9 Bond graph for the model of Fig.8

simply θ but rather

$$\dot{\phi} = \dot{\theta} + \frac{\dot{z}_{gl} - \dot{z}_{gr}}{c}. \quad (24)$$

Eq.(6) is replaced by

$$V = \dot{y}_{us} + h_{rc}\frac{\dot{z}_{gr} - \dot{z}_{gl}}{c}, \quad (25)$$

and

$$\dot{y}_{us} = \dot{y}_s + h'\dot{\theta}. \quad (26)$$

When these relationships are incorporated into the bond graph of Fig.6, the bond graph of Fig.9 results. We note that this version of the model contains both the suspension forces F_{SL} and F_{SR} and the tire normal loads F_{NL} and F_{NR}.

Fig.10 shows a comparison of the step responses of the tire normal forces to a lateral acceleration for the zero roll center height case of Figs.3 and 4 and the finite roll center height case of Figs.8 and 9. Note that now the load transfer in the steady state is identical since we assume the height of the mass center above the road is identical, but the initial responses are quite different. Since the roll-center-

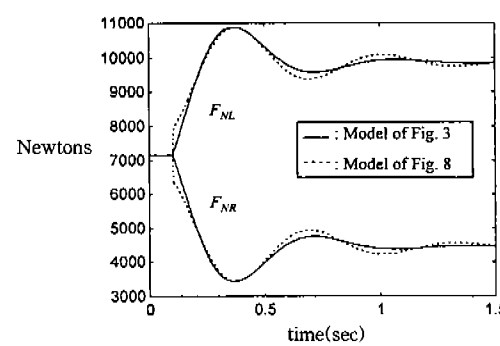

Fig.10 Comparison of tire normal forces after step in lateral acceleration for model of Fig.3 and of Fig.8(Bond graphs of Fig.4 and Fig.9)

axle structure which is incorporated in Figs.8 and 9 is assumed to be massless, the step in lateral acceleration produces an immediate step in load transfer due to a sudden appearance of a lateral force at the roll center. The remaining part of the load transfer is achieved only after the body attains a steady roll angle and the springs are compressed and extended. This simple model points out that load transfer associated with roll center height occurs more rapidly than load transfer associated with roll dynamics.

5. Introduction of Unsprung Mass Dynamics

An advantage of bond graph modeling is that it is often possible to develop a complex model in stages adding effects as they appear necessary. Many possible algebraic problems can be seen in advance of any analytical or computational study by means of a simple causal analysis.

As an example, consider the model of Fig.11 in which wheel masses and tire springs have been incorporated. The bond graph of Fig.12 for this model is a straight-forward extension of Fig.9. The causal analysis of this system shows that no algebraic loops or implicit equations will be necessary in writing the equations of motion.

Fig.13 shows simulation results using parameters from Table 1. The inputs again are steps in lateral acceleration and now

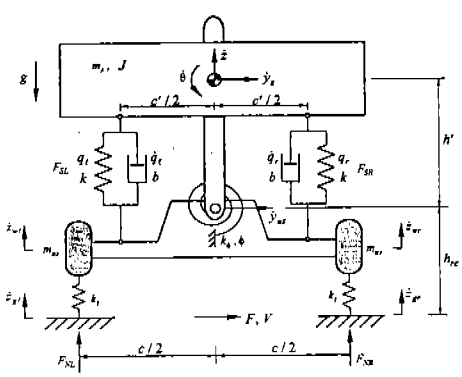

Fig.11 Model including unsprung mass dynamics

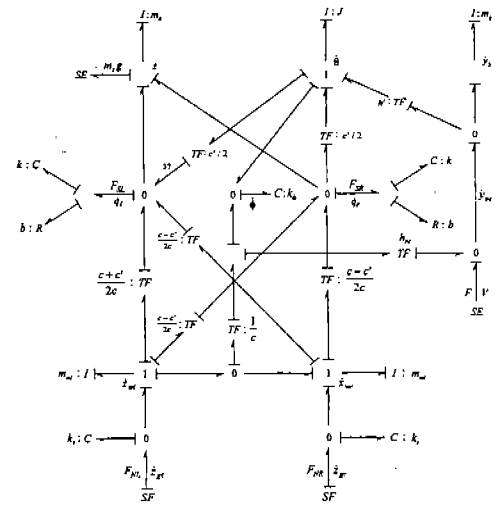

Fig.12 Bond graph for the model of Fig.13

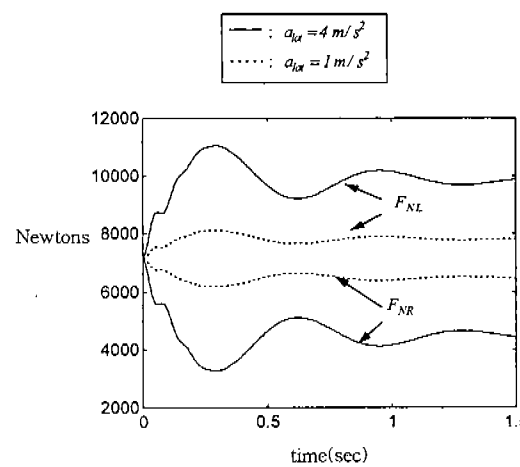

Fig.13 Normal loads for model of Fig.11 and bond graph of Fig.12 in response to step changes in lateral acceleration

one can clearly see load transfer due to roll center height which occurs rapidly but no longer instantaneously as in Fig.10 due to the unsprung mass dynamics. The main body roll dynamics are again evident and the steady state load transfer is approached as the roll oscillations die down.

On the other hand, the lateral motion of the unsprung masses has not been associated with any inertia effect. The bond graph shows clearly that if this is done, derivative causality and implicit rather than explicit differential equations will result. (To see this, imagine inserting an I-element on a 1-junction on either of the bonds on which V or $\dot{y}_{us}$ appear.) One could decide that this was necessary and to define a center of mass velocity for the unsprung mass, or, more simply to augment the body mass used to find $\dot{y}_s$ by the unsprung mass. This minor problem is due to the rigid pivot point assumed at the roll center. A much more complex model without derivative causality could also be derived by assuming some lateral compliance at the roll center pivot. There is no definite answer about what approach to take since engineering judgment must be used based on the purpose of the model.

6. Alternative Suspension Linkage

Fig.14 shows a modified type of suspension which includes a linkage from the wheel to the body. This is just one of a number of possible linkage systems which in one way or another relate the relative velocities across springs and dampers to motions of the wheels and the body. In this example, the spring and damper relative velocities are different and can be

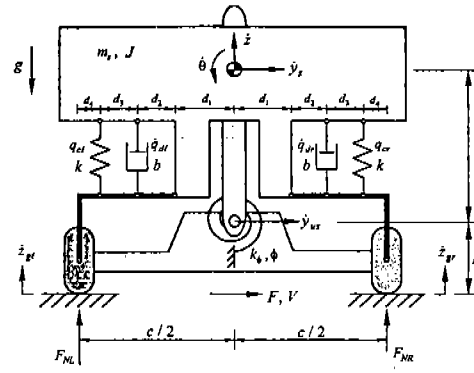

Fig.14 Model with alternative type of suspension linkage

found to be functions of $\dot{z}$, $\dot{\theta}$, and the wheel vertical velocities $\dot{z}_{gl}$ and $\dot{z}_{gr}$ using standard methods described in Ref.[5] Once this has been done, and the kinematic relationships have been incorporated into the system bond graph using either multi-port transformers or 2-port transformer structures as was done in the previous figures, there is no need to analyze the linkage forces since the bond graph will incorporate the necessary force transformations automatically. Nonlinear linkage relations will simply require displacement modulated transformers.

7. Conclusions

The bond graph models have shown some facts known to some but not understood by many :

1) Simple combinations of ride and handling models as shown in Figs.1 and 2 implicitly assume that roll centers are at ground level. For most suspension types this is not the case.
2) The load transfer has to do with two phenomena. The suspension, reacting to roll angle and roll rate does ge-

nerate a moment contributing to load transfer. A lateral force acting at the roll center also contributes to the load transfer. In steady turns, only the total height of the center of mass above the roadway, the lateral acceleration and the track width determine the load transfer. Unless the roll angle is extreme enough to shift the center of gravity significantly, the roll angle does not affect the steady state load transfer.

3) For a four wheel vehicle the total load transfer is essentially predictable using the same concepts studied in the half-car model. However the distribution of load transfer between the front and rear axles depends upon differences between the front and rear suspension systems. This distribution of load transfer(both in the steady state and in the transient state(is important for the handling properties of the vehicle. The type of models discussed here can be extended readily to the complete vehicle.
4) Bond graph techniques assure compatibility between assumptions about force balances and about velocity constraints through use of power conserving transformations represented by junction structures.
5) Bond graphs and variational methods often neglect workless constraint forces. Assuming a finite velocity associated with such forces allows the forces to appear in the bond graph. The forces are then available even if the velocities are actually assumed to vanish.

References

1. Bundorf, R.T., "The Influence of Vehicle Design Parameters on Characteristic Speed and Understeer", *SAE Paper 670078*, 1967.
2. Gillespie, T.D., "Fundamentals of Vehicle Dynamics", *The Society of Automotive Engineers*, 1992.
3. Milliken, W.F. and Millian, D.L., "Race Car Vehicle Dynamics", *The Society of Automotive Engineers*, 1995.
4. Blank, J. J., "Active Controls Used for Enhancement of Maneuverability and Handling Predictability of Automobiles", *Ph.D. Thesis*, Department of Mechanical and Aeronautical Engineering, The University of California, Davis, 1995.
5. Karnopp, D.C., Margolis, D.L., and Rosenberg, R.C., "*System Dynamics: A Unified Approach*", John Wiley & Sons, New York, 1990.
6. Crandall, S.H., Karnopp, D.C., Jurtz, E. F., Pridemore-Brown, D.C., "Dynamics of Mechanical and Electromechanical Systems", *McGraw-Hill, New York*, 1968.